Reinforced Transport Kinetics and Structural Stability of Micron-Si Anode In PVDF-Based Composite Solid-State Batteries via Single-Walled Long Carbon Nanotubes

Zikai Li [1], Tong Zhang [1], Zixuan Fang [1], Haiping Zhou [1] and Mengqiang Wu [1, *]

[1] School of Materials and Energy, University of Electronic Science and Technology of China, Chengdu, 611731, China.

Abstract. Silicon-based anode solid‐state batteries are among the most promising systems for simultaneously achieving high energy density and enhanced safety. However, silicon anodes suffer from severe loss of electronic contact in low–electrolyte or electrolyte‐free environments due to their substantial volume changes, which significantly hinders their integration into solid‐state systems. In this work, we introduce single-walled long carbon nanotubes (SWCNTL) into micron-sized silicon (MSi) anodes to reinforce the three‐dimensional conductive network and thus optimize electrochemical performance in a solid‐state system based on poly(vinylidene fluoride)@lithium lanthanum zirconium tantalum oxide (PVDF@LLZTO)composite solid electrolyte. We demonstrate that SWCNTL promote deeper lithiation of MSi particles at elevated current densities, while simultaneously enhancing electron‐ion transport kinetics and mechanical integrity during cycling under solid-state conditions. Thus, MSi electrodes incorporating SWCNTL deliver markedly improved electrochemical performance and cycling stability in both PVDF@LLZTO-based solid-state half-cells and solid-state full cells countered with $LiFePO_4$(LFP)cathode. Our findings provide a viable strategy to enhance the practical application of silicon anodes in next-generation solid-state battery systems.

Keywords: PVDF and LLZTO Composite Solid-state batteries; Micron Silicon anode; Reinforced Transport Kinetics; Single Walled Long Carbon nanotubes.

1. Introduction

Solid state electrolyte has caught attention due to safety concerns with growing needs of high energy density materials for Li^+ ion batteries[1, 2]. Organic/inorganic composite solid electrolyte stands out with combined advantages provided by mechanically-superior, polymeric constituent and ion-transport profitable, ceramic constituent[2]. In addition, MSi is of great potential in the pursuit of boosting energy storage performance due to its tremendous specific capacity (3580 mAh/g, over 10 times higher than commercial graphite), lower surface area to alleviate side reaction than nano-sized silicon and dependable economic feasibility[1, 3, 4]. However, severe volume exchange (400%) hinders wider appliance of MSi with catastrophic electrical contact failure by colossal, unevenly distributed inner/internal stress particularly in solid-state batteries, where the interface between the solid electrolyte and Si anode goes fragile during cycling[5].

To address these problems, researchers have dived into several methods such as porous structural construction, carbon-compositing, novel electrolyte and binder design[5, 6]. Among these strategies, the preservation of the integrity of the electrode's conductive network and the assurance of long-term electrical contact have retained substantial foundation in liquid electrolyte battery systems[7-11]. However, further investigation is still required to deepen our understanding of maintaining electrical contact in silicon anodes within solid-state batteries. In our previous work, we developed a PVDF@LLZTO organic–inorganic composite solid electrolyte that exhibits high ionic conductivity, uniform dispersion of organic and inorganic phases with excellent processability[12]. Herein, we conducted an in-depth study on the differences in electrical contact behavior between the MSi anode active material and two conductive additives—Super P (SP) and SWCNTL—in a solid-state battery system. Utilizing Differential Capacity vs. Voltage (dQ/dV)

analysis, Electrochemical Impedance Spectroscopy (EIS), and Scanning Electron Microscopy (SEM), we observed that the incorporation of SWCNTL not only significantly promoted the alloying reaction of MSi but also markedly enhanced the capacity retention and rate performance of the MSi anode. These improvements further contributed to the cycling stability of the MSi–LFP full cell in the solid-state battery configuration. Our findings underscore the efficacy of employing long single-walled carbon nanotubes to optimize the conductivity network stability of the MSi anode by ensuring effective electrical contact and promoting electron/ion transport kinetics within electrode.

2. Experimental Section

2.1 Materials preparation

2.1.1 Fabrication of PVDF@LLZTO membrane

Based on our previous work, the preparation of the PVDF@LLZTO composite solid-state electrolyte follows the same procedure as described earlier. In brief, poly(vinylidene fluoride-co-chlorotrifluoroethylene) (PVDF-CTFE) is blended with lithium lanthanum zirconium tantalum oxide (LLZTO) and lithium bis(fluorosulfonyl)imide (LiFSI) in N,N-dimethylformamide (DMF) solvent. The mixture is thoroughly stirred to ensure uniform dispersion. Subsequently, the slurry is cast onto a polytetrafluoroethylene (PTFE) template using a casting method.

2.1.2 Fabrication of electrodes

The MSi anode is prepared by mixing the active material, polyacrylic acid (PAA) binder, and conductive additives in a weight ratio of 8:1:1 using the casting method. In the experimental group, the conductive additive comprises 10 wt% long single-walled carbon nanotubes (SWCNTL), while the control group uses pure Super P (SP). The active material loading is ~ 0.6 mg/cm².

The LFP cathode is fabricated by mixing the active material, polyvinylidene fluoride (PVDF) binder, and SP conductive additive in a weight ratio of 9:0.5:0.5 using the casting method. The active material loading is approximately 5 mg/cm², with a nominal N/P ratio of 1.1 ~ 1.2 for the full cell.

2.2 Electrochemical measurement

All coin-type cells were assembled in an argon-filled glove box. Commercial LB-535 electrolyte was used for cell assembly and 7.5 uL for each side so as to improve interfacial wettability. The half-cell voltage range was 0.01–1.5 V, with a current density of 0.25 C (1 C = 3580 mAh/g); the full-cell voltage range was 2.5–3.6 V, with a current density of 0.2 C (1 C = 170 mAh/g). Electrochemical impedance spectroscopy (EIS) measurements were conducted over a frequency range of 1 MHz to 0.01 Hz. The ionic conductivity (σ) of the solid polymer electrolyte was calculated using the following formula:

$$\sigma = L/(RS) \quad (1)$$

where L is the thickness of the solid polymer electrolyte, R is the high-frequency intercept obtained from the EIS measurement, and S is the surface area of the electrode. The high-frequency intercept corresponds to the solution resistance (R_s), which is determined from the Nyquist plot. The thickness L and surface area S are measured directly.

3. Results and Discussion

To elucidate the structural characteristics of the PVDF@LLZTO composite solid-state electrolyte, X-ray diffraction (XRD) analysis was performed, as in Fig. 1(a). The XRD pattern of LLZTO powder exhibits diffraction peaks that closely match the standard JCPDS card #45-0109, indicating a pure cubic phase of the garnet-type structure. This confirms the high purity of the LLZTO powder used in our study. The corresponding spectrum of PVDF@LiFSI exhibits two weak peaks at 36.4° and 39.2°, a broad characteristic peak at about 20.1° and a small peak at 22.1°, which

verified the semi-crystalline phase of the polymer matrix. PVDF@LLZTO has combined peak identities of PVDF and LLZTO without other peak, which indicates the successful fabrication of PVDF@LLZTO electrolyte.

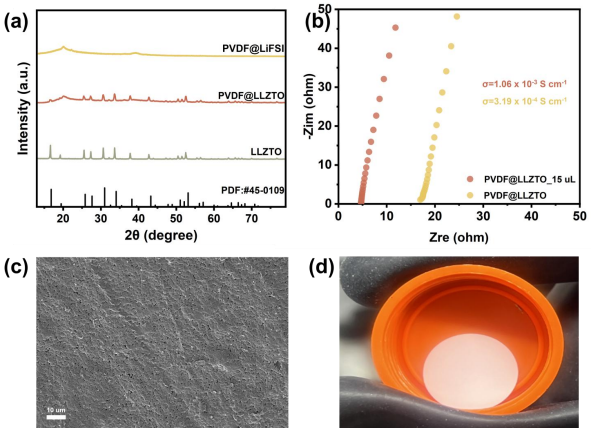

Fig. 1 Morphology and conductivity of PVDF@LLZTO

Fig. 1(b) shows the ionic conductivity of the PVDF@LLZTO electrolyte. Even without any liquid electrolyte, it exhibits a respectable ionic conductivity of 3.19×10^{-4} S m^{-1}, which increases to 1.06×10^{-3} S m^{-1} after infiltration with 15 μL of liquid electrolyte, demonstrating its ability to facilitate efficient ion transport. Fig. 1(c) presents the SEM image of PVDF@LLZTO, revealing a smooth surface that promotes good interfacial contact with the electrode. Fig. 1(d) shows an optical photo of the PVDF@LLZTO membrane, which is an opaque white film.

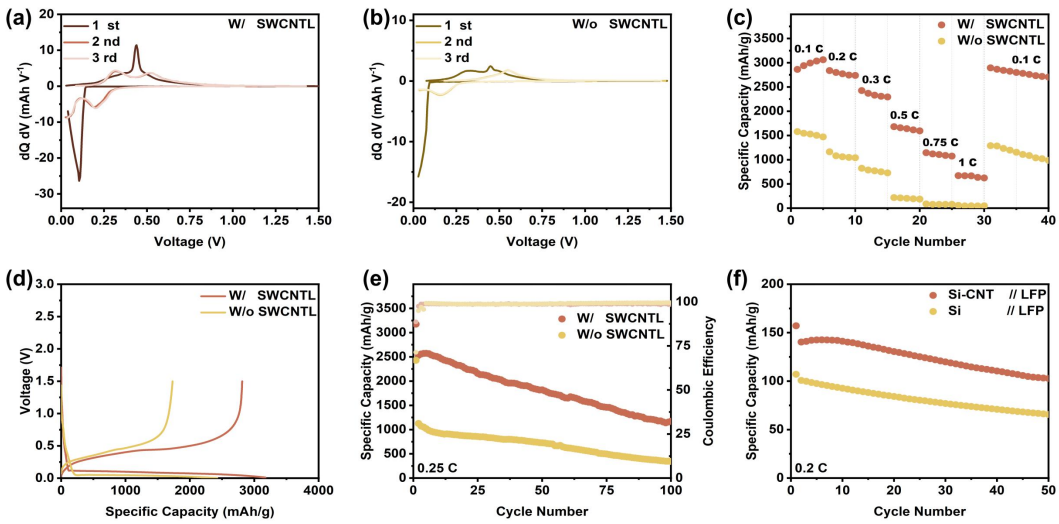

Fig. 2 Electrochemical performance of MSi anode with or without SWCNTL in Solid-state batteries

To thoroughly investigate the influence of single-walled carbon nanotubes (SWCNTL) on the electrochemical behavior of MSi anodes, we conducted galvanostatic charge–discharge cycling tests at a current density of 0.25 C on both the experimental group containing SWCNTL (denoted as W SWCNTL) and the control group without SWCNTL (denoted as W/o SWCNTL). The differential capacity (dQ/dV) curves for the first three cycles are presented in Fig. 2(a) and 2(b). During the initial cycle, activated at 0.05 C, both groups exhibited a reduction peak around 0.1 V and oxidation peaks near 0.31 V and 0.44 V. Notably, the control group displayed a partial reduction peak approaching 0 V, indicating electrochemical interruption despite available lithium storage capacity. In contrast, the experimental group demonstrated two distinct reduction peaks at approximately 0.1 V and 0.2 V, corresponding to oxidation peaks at 0.32 V and 0.51 V, respectively. These observations suggest that the experimental group undergoes two phase transitions: crystalline silicon (c-Si) to amorphous lithium-silicon alloy (a-Li_xSi) and further lithiation of a-Li_xSi. The

control group, however, appears to experience only the a-Li_xSi phase transition. This indicates that the addition of SWCNTL enhances the lithium-ion transport kinetics in the MSi anode, facilitating more efficient electrochemical reactions. Fig. 2(c) illustrates the rate performance of half-cells from both groups tested at current densities ranging from 0.1 C to 1 C. The experimental group exhibited significantly superior rate capability, maintaining a discharge capacity of 670 mAh/g at 1 C. Upon returning to 0.1 C, the capacity recovered to its initial value, whereas the control group showed negligible capacity after 0.5 C. These results confirm that incorporating SWCNTL effectively improves the rate performance of MSi anodes in solid-state batteries. Fig. 2(d) and 2(e) present the first charge–discharge curves and cycling performance of half-cells from both groups at a current density of 0.25 C. The experimental group achieved a first discharge capacity of 3174 mAh/g with a Coulombic efficiency of 88.6%, compared to 2427 mAh/g and 71.3%, respectively, for the control group. After 100 cycles, the experimental group retained a capacity of 1171 mAh/g, while the control group maintained only 343 mAh/g. These findings underscore the significant role of SWCNTL in enhancing the capacity retention of MSi anodes in solid-state systems. Furthermore, to assess the influence of SWCNTL on the electrochemical behavior of MSi in full-cell configurations, we assembled MSi anodes with $LiFePO_4$ (LFP) cathodes and tested them at 0.2 C. As shown in Fig. 2(f), the experimental group demonstrated a discharge capacity of 102.7 mAh/g after 50 cycles, whereas the control group exhibited only 65.6 mAh/g. This further corroborates that the addition of SWCNTL enhances the lithiation capability of MSi anodes in solid-state batteries.

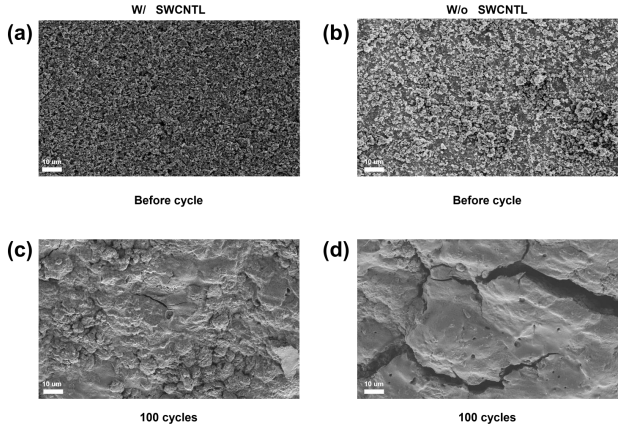

Fig. 3 SEM images of MSi anode before and after 100 cycles in solid-state half cell

To investigate the impact of SWCNTL on the mechanical integrity of MSi anodes during cycling, we conducted SEM imaging of the electrodes before and after 100 charge–discharge cycles. Fig. 3(a) and 3(b) present the SEM images of the electrodes from the experimental group (W SWCNTL) and the control group (W/o SWCNTL) before cycling, respectively. Both electrodes exhibit uniform distribution of MSi particles, indicating well-dispersed active materials. Fig. 3(c) and 3(d) show the SEM images of the electrodes from the experimental and control groups after 100 cycles. The experimental group maintains a relatively smooth surface with only fine cracks; In contrast, the control group exhibits deeper and wider cracks, indicating more significant mechanical degradation, suggesting that the addition of SWCNTL enhances the structural stability of the MSi anode during cycling.

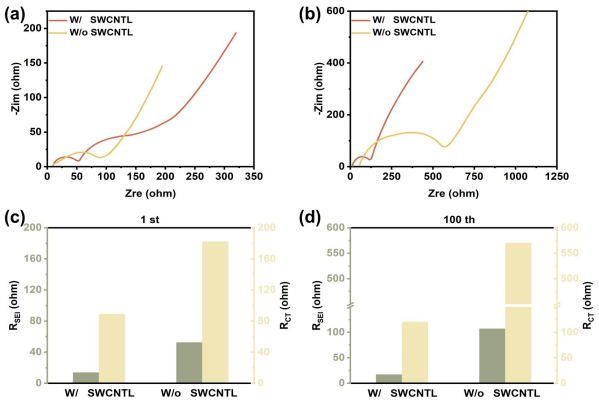

Fig. 4 EIS curves of MSi anode after 1 and 100 cycles in solid-state half cell

To clarify the impact of SWCNTL on ion-transport behavior in MSi during cycling, impedance spectra of solid-state half-cells from both experimental and control samples were acquired after 1 and 100 cycles. Fig. 4(a) presents Nyquist spectra after the first cycle, and Fig. 4(c) compares the extracted charge-transfer resistance (R_{ct}) and SEI resistance (R_{SEI}). After one cycle, the experimental cell exhibits R_{ct} = 13.7 Ω and R_{SEI} = 88.9 Ω, both substantially lower than the corresponding values in the control cell. Following 100 cycles, R_{ct} and R_{SEI} increase moderately to 16.9 Ω and 120.4 Ω in the experimental cell, reflecting significantly smaller growth than in the control. These findings further prove that SWCNTL addition significantly mitigates the progressive growth of interfacial and charge-transfer resistances under cycling, thereby preserving superior ion-transport kinetics in the MSi anode.

4. Summary

In conclusion, we investigate how the addition of SWCNTL improves the 3D conductive network within MSi anodes in PVDF@LLZTO based solid-state battery systems and its consequent impact on electrochemical performance. XRD, Conductivity test and SEM images prove fine fabrication of highly ion-conductive and homogeneous PVDF@LLZTO electrolyte. Analysis of dQ/dV curves and rate performance reveals that the SWCNTL-mediated 3D network facilitates deeper lithiation under higher currents. Moreover, comparative EIS measurements at varying cycle numbers demonstrate that SWCNTL significantly alleviates impedance growth during cycling, ensuring efficient electron and ion transfer. Thus, SWCNTL incorporation is evident to the enhancement of charge and ion transport kinetics, enabling ameliorated capacity deallocation during cycling. SEM images captured before and after cycling further confirm that SWCNTL reinforcement improves electrode structural integrity, resulting in enhanced performance in both solid-state half-cells and MSi ‖ LFP full cells. Collectively, our work provides a robust reference for advancing the practical implementation of silicon anodes in solid-state battery systems.

5. References

[1] BOORBOOR AJDARI F, ASGHARI P, MOLAEI AGHDAM A, et al. Silicon solid state battery: The solid‐state compatibility, particle size, and carbon compositing for high energy density. Advanced Functional Materials, 2024, 34(30): 2314822.

[2] SAND S C, RUPP J L, YILDIZ B. A critical review on li-ion transport, chemistry and structure of ceramic–polymer composite electrolytes for solid state batteries. Chemical Society Reviews, 2024.

[3] SUN L, LIU Y, WANG L, et al. Advances and future prospects of micro‐silicon anodes for high‐energy‐density lithium‐ion batteries: A comprehensive review. Advanced Functional Materials, 2024, 34(39): 2403032.

[4] GU L, HAN J, CHEN M, et al. Enabling robust structural and interfacial stability of micron-si anode toward high-performance liquid and solid-state lithium-ion batteries. Energy Storage Materials, 2022, 52: 547-561.

[5] KHAN M, YAN S, ALI M, et al. Innovative solutions for high-performance silicon anodes in lithium-ion batteries: Overcoming challenges and real-world applications. Nano-Micro Letters, 2024, 16(1): 179.

[6] CHEN X, WANG B, YE Y, et al. Design of electrodes and electrolytes for silicon‐based anode lithium‐ion batteries. Energy & Environmental Materials, 2025, 8(2): e12838.

[7] ZHONG H, LIU D, YUAN X, et al. Advanced micro/nanostructure silicon-based anode materials for high-energy lithium-ion batteries: From liquid-to solid-state batteries. Energy & Fuels, 2024, 38(9): 7693-7732.

[8] ZHANG B, DONG Y, HAN J, et al. Physicochemical dual cross‐linking conductive polymeric networks combining high strength and high toughness enable stable operation of silicon microparticle anodes. Advanced Materials, 2023, 35(29): 2301320.

[9] LI Z, GUO A, LIU D. Water-soluble conductive composite binder for high-performance silicon anode in lithium-ion batteries. Batteries, 2022, 8(6): 54.

[10] SU Y, LV Y, HABIBIPOUR M R, et al. Dynamic stable interface between cnt and nanosilicon for robust anode with large capacity and high rate performance. Energy Storage Materials, 2023, 61: 102892.

[11] HE Z, ZHANG C, ZHU Y, et al. The acupuncture effect of carbon nanotubes induced by the volume expansion of silicon-based anodes. Energy & Environmental Science, 2024, 17(10): 3358-3364.

[12] LUO B, WU J, ZHANG M, et al. Surface modification of garnet fillers with a polymeric sacrificial agent enables compatible interfaces of composite solid-state electrolytes. Chemical Science, 2023, 14(45): 13067-13079.